



1 **Insignificant effects of elevated CO<sub>2</sub> on bacterioplankton**  
2 **community in a eutrophic coastal mesocosm experiment**

3 Xin Lin<sup>†\*1</sup>, Ruiping Huang<sup>†1</sup>, Yan Li<sup>1</sup>, Yaping Wu<sup>1,2</sup>, David A. Hutchins<sup>3</sup>, Minhan Dai<sup>1</sup>,  
4 Kunshan Gao<sup>\*1</sup>

5

6 **Institutions:**

7 <sup>1</sup>State Key Laboratory of Marine Environmental Science, Xiamen University (Xiang An Campus),  
8 Xiamen 361102, China.

9 <sup>2</sup>College of oceanography, Hohai university, No.1 Xikang road, Nanjing 210000, China.

10 <sup>3</sup>Department of Biological Sciences, University of Southern California, 3616 Trousdale Parkway, AHF  
11 301, Los Angeles, CA 90089-0371, USA.

12

13 <sup>†</sup> These authors contribute equally to this work.

14 *Correspondence to:* Xin Lin (xinlinulm@xmu.edu.cn, TEL: +865922880171);

15 Kunshan Gao (ksgao@xmu.edu.cn, TEL: +865922187963)

16

17

18

19

20

21

22

23

24

25

26

27

28

29

30

31

32

33

34

35



1 **Abstract**

2       There is increasing concern about the effects of ocean acidification on marine biogeochemical and  
3 ecological processes and the organisms that drive them, including marine bacteria. Here, we examine the  
4 effects of elevated CO<sub>2</sub> on bacterioplankton community during a mesocosm experiment using an  
5 artificial phytoplankton community in subtropical, eutrophic coastal waters of Xiamen, Southern China.  
6 We found that the elevated CO<sub>2</sub> hardly altered the network structure of the bacterioplankton taxa present  
7 with high abundance but appeared to reassemble the community network of taxa present with low  
8 abundance by sequencing of the bacterial 16S rRNA gene V3-V4 region and ecological network analysis.  
9 This led to relatively high resilience of the whole bacterioplankton community to the elevated CO<sub>2</sub> level  
10 and associated chemical changes. We also observed that the Flavobacteriia group, which plays an  
11 important role in the microbial carbon pump, showed higher relative abundance under elevated CO<sub>2</sub>  
12 condition during the developing stage of the phytoplankton bloom in the mesocosms. Compared to the  
13 CO<sub>2</sub> enrichment, the phytoplankton bloom had more pronounced effects on bacterioplankton community  
14 structure. Our results suggest that the bacterioplankton community in this subtropical, high nutrient  
15 coastal environment is relatively insensitive to changes in seawater carbonate chemistry.

16 **Key words:** elevated CO<sub>2</sub>; mesocosm; bacterioplankton community; ecological network; Flavobacteriia

17

18

19

20

21

22



## 1 **1 Introduction**

2 It is well established that ocean acidification is being caused by increased uptake of  
3 anthropogenically-derived carbon dioxide in the surface ocean. Consequently, it is predicted that under a  
4 “business-as-usual” CO<sub>2</sub> emission scenario, the present average surface pH value will drop 0.4 over the  
5 next century (Gattuso et al., 2015). Despite a growing interest in the importance of the roles of marine  
6 bacterioplankton in ocean ecosystems and biogeochemical cycles, our current understanding of their  
7 responses to ocean acidification is still limited. Over half of autotrophically-fixed oceanic CO<sub>2</sub> is  
8 processed by heterotrophic bacteria and archaea through the microbial loop and carbon pump (Azam,  
9 1998; Jiao *et al.*, 2010). Furthermore, marine bacterioplankton play an essential role in marine  
10 ecosystems and global biogeochemical cycles central to the biological chemistry of Earth (Falkowski et  
11 al., 2008). The null hypothesis is that elevated CO<sub>2</sub> will not affect biogeochemistry processes (Liu *et al.*,  
12 2010; Joint *et al.*, 2011), however more investigation is required. Ocean acidification mesocosm  
13 experiments provide good opportunities to explore the responses of marine organisms, including marine  
14 bacteria, to elevated CO<sub>2</sub>. Mesocosm studies conducted in the Arctic Ocean, Norway, Sweden and the  
15 Mediterranean coastal sea using natural phytoplankton communities have found that elevated CO<sub>2</sub> has  
16 little direct effect on the bacterioplankton community (Zhang et al., 2013; Ray et al., 2012, Roy et al.,  
17 2013; Baltar et al., 2015). In contrast, phytoplankton blooms induced by high CO<sub>2</sub> can sometimes have  
18 significant indirect effects on heterotrophic microbes, thus altering bacterioplankton community  
19 structure (Allgaier et al., 2008).

20 Although most mesocosm studies have showed that elevated CO<sub>2</sub> had an insignificant impact on  
21 bacterioplankton community structure, microcosm experiments have demonstrated that small changes in  
22 pH can have direct effects on marine bacterial community composition (Krause et al., 2012). Ocean



1 acidification experiments using natural biofilms showed bacterial community shifts, with decreasing  
2 relative abundance of Alphaproteobacteria and increasing Flavobacteriales (Witt et al., 2011). Coastal  
3 microbial biofilms grown at high CO<sub>2</sub> level also showed different community structures compared to  
4 those grown at ambient CO<sub>2</sub> level in a natural carbon dioxide vent ecosystem (Lidbury et al., 2012).  
5 Ocean acidification also affects the community structure of bacteria associated with corals. It has been  
6 reported that the relative abundance of bacteria associated with diseased and stressed corals increased  
7 under decreasing pH conditions (Meron et al., 2011). The effects of ocean acidification on isolated  
8 bacterial strains have also been investigated. Under lab conditions, growth of *Vibrio alginolyticus*, a  
9 species belonging to the class Gammaproteobacteria, was suppressed at low CO<sub>2</sub> levels (Labare et al.,  
10 2010). In contrast, stimulation of growth was observed for one Flavobacteriia species under high CO<sub>2</sub>  
11 levels (Teira et al., 2012).

12 Taken together, results from mesocosm, microcosm and cultured isolates experiments indicate a  
13 potentially complex interaction between different groups of marine bacteria in response to elevated CO<sub>2</sub>.  
14 To begin to elucidate these complex interactions, network analysis methods would be beneficial.  
15 Ecological network approaches have been successfully applied to investigate the complexity of  
16 interactions among zooplankton and phytoplankton from different trophic levels in the Tara Oceans  
17 Expedition project (Lima-mendez *et al.*, 2015; Guidi *et al.*, 2015). Previous studies using ecological  
18 network analysis showed that elevated CO<sub>2</sub> significantly impacted soil bacterial/archaeal community  
19 networks, by decreasing the connections for dominant fungal species and reassembling unrelated fungal  
20 species in a grassland ecosystem (Tu et al., 2015). Elucidating the complex interactions between  
21 bacterioplankton and other marine organisms under anthropogenic perturbation will increase our  
22 understanding of their impact in a holistic way.



1 It has been reported that eutrophication problems in coastal regions lead to complex cross-links  
2 between ocean acidification and eutrophication (Cai et al., 2011). The occurrence of ocean acidification  
3 combined with other environmental stressors such as eutrophication can potentially produce synergistic  
4 or antagonistic effects on bacterioplankton that differ from those caused by ocean acidification alone.  
5 Although there are some reports from mesocosm experiments describing the response of bacteria to  
6 elevated CO<sub>2</sub>, there are limited studies on how the bacterial community responds to ocean acidification in  
7 eutrophic coastal seawater. In this study, the response of bacterial community to ocean acidification was  
8 investigated using a mesocosm experiment conducted in a eutrophic coastal area in Xiamen, China using  
9 V3-V4 region of 16S rRNA gene Illumina sequencing. The objective was to explore the effects of ocean  
10 acidification on the bacterioplankton community composition and ecological network structure in a  
11 eutrophic coastal mesocosm experiment.

## 12 **2 Methods**

### 13 **2.1 Mesocosm setup and carbonate system manipulation**

14 The mesocosm experiment was conducted in the FOANIC-XMU (Facility for the Study of Ocean  
15 Acidification Impacts of Xiamen University) mesocosm platform located in Wuyuan Bay, Xiamen,  
16 Fujian province, East China Sea (N24°31'48", E118°10'47") during the months of December 2014 and  
17 January 2015 (Fig. 1). Each transparent thermoplastic polyurethane (TPU) cylindrical mesocosm bag  
18 was 3 m deep and 1.5 m wide (~4000 L total volume). After setting up the mesocosm bags into steel  
19 frames, in situ seawater from Wuyuan Bay was filtered through a 0.01µm water purifying system and  
20 used to simultaneously fill eight bags within 24 hours. The initial in situ seawater pCO<sub>2</sub> in Wuyuan Bay  
21 was about 650 µatm. Wuyuan bay, located in the city centre, is strongly influenced by the human  
22 activities. The decomposition of land-sourced organic compounds is also active in Wuyuan Bay. All



1 these reasons may lead to higher  $p\text{CO}_2$  in Wuyuan bay than that in open ocean. In order to reach the  
2 target low  $p\text{CO}_2$  associated with ambient air (400 ppm),  $\text{Na}_2\text{CO}_3$  was added to each mesocosm to  
3 increase dissolved inorganic carbon (DIC) and total alkalinity (TA) by 100  $\mu\text{mol/L}$  and 200  $\mu\text{mol/L}$   
4 respectively based on the carbonate system calculation (Lewis et al. 1998). To adjust seawater to the end  
5 of this century projected seawater under 1000 ppm  $\text{CO}_2$  condition, about 5 L of  $\text{CO}_2$  saturated filtered  
6 seawater was added to 4 mesocosms (#2, #4, #7, #9) respectively which were considered as the HC  
7 treatment, while the other 4 mesocosms (#1, #3, #6, #8) were considered as the LC treatment.  
8 Throughout the experiment, HC mesocosms and LC mesocosms were bubbled with air containing 1000  
9 ppm and 400 ppm  $\text{CO}_2$ , respectively supplied by  $\text{CO}_2$  Enrichlor (CE-100B, Wuhan Ruihua Instrument &  
10 Equipment Ltd, China) at a flow rate of 4.8 L per minute.

11 Two diatoms, *Phaeodactylum tricornerutum* CCMA 106 (isolated from South China Sea in 2004) from  
12 the Centre for Collections of Marine Bacteria and Phytoplankton of the State Key Laboratory of Marine  
13 Environmental Science (Xiamen University, China), and *Thalassiosira weissflogii* CCMP 102 from the  
14 Provasoli-Guillard National Center for Culture of Marine Phytoplankton (CCMP, USA), as well as the  
15 coccolithophorid *Emiliania huxleyi* (CS-369) from the Commonwealth Scientific and Industrial  
16 Research Organization (CSIRO, Australia) were used as inoculum to construct a model phytoplankton  
17 community. The effects of ocean acidification on these phytoplankton species mentioned above have  
18 been intensively studied in the lab at physiological, biochemical and molecular levels. However, it is  
19 difficult to extrapolate the response of these species to ocean acidification in natural complex  
20 environments based on the lab single species experiments (Busch et al., 2015). In this study, the  
21 artificial phytoplankton were used to further investigate the effects of ocean acidification on these  
22 species in the community and ecosystem levels in the context of mesocosm experiment (Jin et al., 2015;



1 Liu et al., submitted). The initial concentration of *P. tricornutum* and *T. weissflogii* was 10 cells/mL  
2 respectively, and *E. huxleyi* was 20 cells/mL. Although 0.01µm filtered seawater were used in this  
3 mesocosm experiment, the bacterioplankton appeared on day 0. The bacterioplankton in this mesocosm  
4 experiment originated from both the lab culture and the natural seawater. The inoculated algal culture  
5 was also not axenic. The bacteria composition in the inoculated phytoplankton culture is shown in Fig.  
6 S1. The mesocosm and the CO<sub>2</sub> bubbling system were not sterile at the beginning of the experiment and  
7 not completely closed during the experiment. The natural bacterioplankton were undoubtedly introduced  
8 into the mesocosm system through bubbling and air-sea exchange. So the bacterioplankton community in  
9 this mesocosm experiment was derived from the bacteria added inoculated phytoplankton culture and  
10 the natural local prokaryotic assemblage.

## 11 **2.2 Bacteria sampling, filtration and sample selection**

12 A total of 500 ml to 2 L of water, depending on bacterial concentration, was collected from mesocosms.  
13 Six of the mesocosms (HC: #2, #4, #7 and LC: #1, #6, #8) were chosen for further study. Samples from  
14 days 4, 6, 8, 10, 13, 19, and 29 were collected in this study due to time, personnel and equipment  
15 constraints. Sequential size fractionated filtration (2 µm and 0.2 µm polycarbonate filters) by peristaltic  
16 pump was used to filter seawater collected from the mesocosm bags.

## 17 **2.3 DNA extraction, 16S rDNA V3-V4 region amplification and Illumina MiSeq sequencing**

18 Samples collected by 0.2 µm polycarbonate filter as described above were washed with PBS buffer then  
19 centrifuged at 9600g to obtain a cell pellet. A previously described DNA extraction protocol was utilized  
20 (Francis et al., 2005). Amplification, library construction and sequencing were performed offsite at  
21 ANNOROAD using the DNA samples isolated as described above. Primers were 341F  
22 (5'-CCTACGGGNGGCWGCAG-3') and 805R (5'-GACTACHVGGGTATCTAATCC-3'), targeting



1 the V3-V4 hyper variable regions of bacterial 16S rRNA gene. The PCR amplification condition was as  
2 follows: initial denaturation at 95°C for 3 min, 25 cycles of denaturation at 95°C for 30 s, annealing at  
3 55°C for 30 s and extension at 72°C for 30 s, then final extension at 72°C for 5 min. DNA library  
4 construction and sequencing followed the MiSeq Reagent Kit Preparation Guide (Illumina, USA).

#### 5 **2.4 Sequence assignment and sequence statistics analysis**

6 Clean paired-end reads were merged using PEAR (Zhang et al., 2014). The remaining raw sequences  
7 were distinguished and sorted by unique sample tags. Unique operational taxonomic units (OTUs) were  
8 picked against Greengenes database ([http://greengenes.lbl.gov/cgi-bin/JD\\_Tutorial/nph-16S.cgi](http://greengenes.lbl.gov/cgi-bin/JD_Tutorial/nph-16S.cgi))  
9 (McDonald et al., 2012) at 97% identity. OTUs with less than 2 reads were not considered. QIIME 1.8.0  
10 was used for sequence analysis including OTUs extraction for bacterioplankton community structure  
11 analysis, OTUs overlapping analysis, phylogenetic analysis, species diversity and species richness  
12 analysis, Principal Components Analysis (PCA) (Caporaso et al., 2010). Bacterioplankton community  
13 composition differences were assessed by Unweighted UniFrac distance using QIIME 1.8.0 as well.  
14 Dissimilarity tests were based on the Bray-Curtis dissimilarity index using analysis of similarities  
15 (ANOSIM) (Clarke, 1993), non-parametric multivariate analysis of variance (ADONIS) (Anderson,  
16 2001), and multi-response permutation procedures (MRPP) (Mielke, 1981). Observed species, Chao  
17 index, Shannon index and Simpson index were used for estimating the community diversity. Analysis of  
18 variance (ANOVA) followed by a T-test was performed to determine any significant differences between  
19 HC and LC treatments.

#### 20 **2.5 Ecological network construction and analysis**

21 As previously described, ecological network analysis were performed to do ecological network  
22 construction and analysis based on relative abundance of OTUs in HC and LC treatments with three





1 biological replicates (<http://129.15.40.240/mena/>). Firstly, a similarity matrix was created using Pearson  
2 correlation coefficient across time series by a random matrix theory (RMT)-based approach. Cut-off  
3 values were determined according to  $R^2$  of power-law larger than 0.8 and equal between two  
4 manipulations to construct network structure. In order to ensure the constructed networks were not  
5 random biologically meaningless networks, 100 networks from the same matrix were constructed and  
6 randomized. This resulted in the experimental networks being different from random networks judging  
7 by significantly higher modularity, clustering coefficient and geodesic distance (Table 1). Then, module  
8 separation was produced using greedy modularity optimization, and  $Z$ - $P$  values for all nodes were  
9 calculated. In addition, to compare networks, the network connection was randomly rewired and network  
10 topological properties were calculated. Finally, the bacteria network interaction was visualized by  
11 Cytoscape v.3.3.0. The  $Z$ - $P$  plots were constructed based on within-module ( $Z$ ) and among-module ( $P$ )  
12 values of each node derived from ecological network analysis. Ecological network analysis is a novel  
13 RMT-based framework for studying microbial interactions. A node in ecological network analysis shows  
14 an OTU and a link demonstrates a connection between two OTUs. The shortest path between nodes is  
15 indicated by geodesic distance. Since the network constructed by OTUs can be separated into several  
16 communities, or modules, the modularity value indicates how well a network can be divided into  
17 different communities. Clustering coefficients demonstrate how well a OTU is connected with other  
18 OTUs, while average clustering coefficients indicate the extent of connection in a network.

19

## 20 **3 Results**

### 21 **3.1 Environmental parameters and experimental timeline**

22 The initial inorganic nitrogen,  $\text{PO}_4^{3-}$ , and  $\text{SiO}_3^{2-}$  concentrations were 70–75  $\mu\text{mol/L}$ , 2.5–2.6  $\mu\text{mol/L}$ , and



1 38–39  $\mu\text{mol/L}$ , respectively. Because of the high nutrient levels, the effects of eutrophication cannot be  
2 ignored in this ocean acidification mesocosm experiment. Except  $\text{SiO}_3^{2-}$ , the other nutrient  
3 concentrations decreased with rapid growth of the phytoplankton and reached to low concentrations on  
4 day 15. The dissolved total inorganic nitrogen dropped from initial  $74.9 \pm 2.87 \mu\text{mol/L}$  to  $57.2 \pm 4.37$   
5  $\mu\text{mol/L}$  in the HC condition and  $72 \pm 5.90 \mu\text{mol/L}$  to  $53.6 \pm 5.60 \mu\text{mol/L}$  in the LC condition by day 8,  
6 and then reached low concentrations on day 15 (average  $3\mu\text{mol/L}$  in LC and average  $6\mu\text{mol/L}$  in HC )  
7 The  $p\text{CO}_2$  in this study was calculated from DIC and pH by CO2SYS Program (Lewis et al. 1998).  
8 The initial  $p\text{CO}_2$  of  $373.0 \pm 43.9 \mu\text{atm}$  in the LC treatment and  $1296.0 \pm 159.6 \mu\text{atm}$  in the HC treatment  
9 increased and reached the peak value of  $922.5 \pm 142.0 \mu\text{atm}$  in the LC treatment on day 8 and  $1879.6 \pm$   
10  $145.4 \mu\text{atm}$  in the HC treatment on day 4. After reaching the peak, the  $p\text{CO}_2$  values of both treatments  
11 decreased and were no longer statistically different from day 13 due to rapid  $\text{CO}_2$  uptake by the  
12 phytoplankton, despite air containing 1000 ppm  $\text{CO}_2$  being continuously bubbled into the HC treatments  
13 (Fig. 2). *P. tricornutum* and *T. weissflogii* were the dominant species throughout the whole  
14 phytoplankton bloom in both HC and LC conditions. Chlorophyll *a* (Chl*a*) concentration and diatom cell  
15 densities were used to identify changes in the diatom bloom following inoculation (Fig. 2, Nana Liu et  
16 al., submitted). Chl*a* concentration increased from  $0.23 \pm 0.12 \mu\text{g/L}$  to  $5.33 \pm 1.82 \mu\text{g/L}$  in the LC  
17 conditions, and from  $0.19 \pm 0.07 \mu\text{g/L}$  to  $5.75 \pm 1.17 \mu\text{g/L}$  in the HC conditions from day 4 to day 9.  
18 Thereafter, Chl*a* concentration increased significantly and peaked at  $109.9 \pm 38.04 \mu\text{g/L}$  in the LC  
19 treatment and  $108.6 \pm 46.07 \mu\text{g/L}$  in the HC treatment on day 15. Subsequently, Chl*a* concentrations in  
20 both treatments were maintained at high concentrations until day 25 and decreased progressively  
21 afterward. The bloom process identified by cell concentration of *P. tricornutum* and *T. weissflogii* was  
22 similar with that illustrated by Chl*a* concentration. The growth of these two diatom species entered into



1 logarithmic phase from day 2. Cell density reached highest concentration on day 15 and day 19 for *T.*  
2 *weissflogii* and *P. tricorutum* respectively, and then dropped down slowly. The comprehensive analysis  
3 of phytoplankton cell density, Chla concentration, particle organic carbon (POC) and particle organic  
4 nitrogen (PON) during the experiment were described in Nana Liu et al., submitted.

### 5 **3.2 Overview of sequencing analysis**

6 Following sequencing, 828524 high quality sequences were kept after processing, and 39.3% of  
7 assembled reads were successfully aligned with the database. As a result, a total of 4992 OTUs were  
8 generated after clustering at a 97% similarity level, and 466 OTUs of them were unique. 49.1% of OTUs  
9 were classified to genera level with high taxonomic resolution. The phylogenetic tree was constructed  
10 based on the sequences derived from all of the samples (Fig. S2). The bacterioplankton from all of the  
11 samples in this study were identified as members of Bacteroidetes or Proteobacteria phylums. The most  
12 dominant OTUs were Alphaproteobacteria, Rhodobacterales, Rhodobacterceae and Sediminicola at  
13 class, order, family and genus level respectively (Fig. S3). The most abundant sequences at class, order,  
14 family and genus levels accounted for 43.4 %, 42.6 %, 41.7% and 32.8 % of all sequences respectively.

### 15 **3.3 Bacterioplankton community structure throughout the phytoplankton bloom**

16 Bacterioplankton community structure underwent dynamic changes during the diatom bloom in both the  
17 HC and LC treatments. The bacterioplankton community structure of all samples in different taxonomic  
18 levels is illustrated in Fig. 3. Significant variation in community structure was observed through the  
19 whole diatom bloom process, suggesting that the diatom bloom is a major driver for bacterioplankton  
20 community structure dynamics in both the HC and LC treatments. At the phylum level, the  
21 bacterioplankton were dominated by Proteobacteria, while the relative abundance of Bacteroidetes was  
22 very low when nutrients were replete and diatom biomass was not high. However, Bacteroidetes



1 increased dramatically when diatom biomass increased dramatically, and began to drop down after  
2 reaching a peak on day 10 (Fig. 3 and Fig. 4). In contrast, Proteobacteria began to increase after reaching  
3 its lowest concentration on day 10.

4 The Alphaproteobacteria, Flavobacteriia, and Gammaproteobacteria classes with high abundance in  
5 all samples were selected for further analysis. The proportion of the Gammaproteobacteria class from the  
6 Proteobacteria phylum was very high at the beginning of the experiment ( $50.2 \pm 13.8$  % in the HC  
7 treatment and  $44.1 \pm 6.4$  % in the LC treatment on day 6) and decreased throughout the duration of the  
8 experiment. On the other hand, the Alphaproteobacteria class, also from the Proteobacteria phylum,  
9 decreased from initial high proportions ( $46.9 \pm 13.2$  % in the HC treatment and  $43.9 \pm 11.6$  % in the LC  
10 treatment) on day 6 to low proportions on day 10 ( $27.2 \pm 2.8$  %) in the HC treatment whereas remained  
11 almost unchanged ( $44.6 \pm 7.5$  %) in the LC treatment and increased to  $63.2 \pm 27.3$  % in the HC treatment  
12 and  $60.8 \pm 32.7$  % in the LC treatment on day 29 (Fig. 3 and Fig. 4). The relative abundance of the  
13 Flavobacteriia class from the Bacteroidetes increased from the beginning and reached a peak on day 10  
14 ( $52.2 \pm 4.2$  % in the HC treatment and  $24.8 \pm 16.9$  % in the LC treatment), then dropped down until day  
15 19 ( $19.9 \pm 2.2$  % in the HC treatment and  $18.0 \pm 15.4$  % in the LC treatment) (Fig. 3 and Fig. 4). The  
16 proportional variation of the Flavobacteriales order and the Rhodobacterales order showed similar trends  
17 with the Flavobacteriia class and the Alphaproteobacteria class, respectively, as shown in Fig. 3 and Fig.  
18 4.

### 19 **3.4 The effects of elevated CO<sub>2</sub> on bacterioplankton community structure**

20 Bacterial community structures of the HC and LC treatments were compared at different sampling  
21 time-points. Briefly, CO<sub>2</sub> treatment was not a strong influence on bacterioplankton community structure,  
22 compared to the diatom bloom process (Fig. 3). A dissimilarity test based on ANOSIM, MRPP and



1 ADONIS methods showed that no statistically significant differences were observed between HC and LC  
2 treatments at different time-points (Table 2). PCA analysis also agreed with the dissimilarity test (Fig.  
3 S6). The bacterioplankton community diversity in all samples was estimated by observed species, Chao  
4 index, Shannon index and Simpson index. Rarefaction curves showed no remarkable differences in in  
5 community diversity between HC and LC, regardless of the time point (Fig. S4). In general, the variation  
6 of the bacterioplankton community diversity in both HC and LC treatments followed the same trend,  
7 peaked on day 10 and declined for the remainder of the experiment (Fig. S5).

8 Although the general trend of bacterioplankton community structure variation was similar in both the  
9 HC and LC treatments as described above, some groups of bacterioplankton showed different responses  
10 to elevated CO<sub>2</sub> at some time points. Notably, Bacteroidetes, predominated by the Flavobacteriia had a  
11 higher average proportion in the HC treatment (52.2 % of Bacteroidetes and 52.2 % of Flavobacteriia)  
12 than that in the LC treatment (25.2% Bacteroidetes and 24.8% Flavobacteriia) at the early stage of the  
13 diatom bloom on day 10 ( $p=0.049$  and  $0.053$  respectively). In contrast, Proteobacteria, especially the  
14 Alphaproteobacteria were observed to have lower proportion in the HC treatment (47.8 % of  
15 Proteobacteria and 27.2% of Alphaproteobacteria) than in the LC treatment (74.8 % of Proteobacteria  
16 and 44.6% of Alphaproteobacteria) on day 10 ( $p=0.049$  and  $0.019$  respectively, Fig. 4). At a higher  
17 taxonomic level, Flavobacteriales, demonstrated higher proportions in the HC treatment (52.2 %)  
18 compared to the LC treatment (24.8 %) on day 10 ( $p=0.053$ ), while for Rhodobacterales the inverse  
19 pattern was observed ( $p=0.020$ ). Moreover, Flavobacteriaceae were observed to have a relatively higher  
20 ratio in the HC treatment (50.3 %) compared to the LC treatment (24.0 %) on day 10 ( $p=0.053$ ), whereas  
21 Rhodobacteraceae demonstrated the opposite pattern ( $p=0.021$ , Fig. 4). It is notable that  
22 Alteromonadales, belonging to the Gammaproteobacteria, had a higher ratio in the HC treatment



1 compared to the LC treatment on day 19 and day 29, although it was not statistically significant ( $p=0.24$   
2 and 0.34 on day 19 and 29 respectively).

### 3 **3.5 The effects of elevated CO<sub>2</sub> on bacterioplankton community interactions**

4 Both HC and LC networks were dominated by Alphaproteobacteria, Gammaproteobacteria and  
5 Flavobacteria, suggesting their vital roles in maintaining stability of microbial ecosystems under both  
6 HC and LC conditions. The observation of more negative links compared to positive links indicates the  
7 dominant relationship among bacterioplankton is competitive rather than mutualistic under both the HC  
8 and LC treatments. Average connectivity and average clustering coefficient of the network under the HC  
9 treatment were higher than under LC treatment, while geodesic distance and modularity value was higher  
10 under the LC treatment. Bacterioplankton formed more modules under the LC treatment, but were  
11 densely connected in less modules under the HC treatment (Table 1, Fig. 5). However, as it shown in Fig.  
12 5, the links among the abundant OTU 558885 (Rhodobacteraceae), 572670 (Rhodobacteraceae), 190052  
13 (Flavobacteriaceae), 107130 (Flavobacteriaceae) and 4331023 (Rhodobacteraceae) were positive in both  
14 HC and LC.

15 Interestingly, some nodes that were sparsely distributed in independent modules in the LC network  
16 formed dense modules with high connectivity in the HC network (Fig. 5). As the OTUs connected within  
17 a module, they could be considered as a putative bacterioplankton ecological niche (Zhou et al., 2010). It  
18 is plausible that elevated CO<sub>2</sub> disrupted the connection between different bacterioplankton community  
19 niches, but enhanced alternative connections among species within certain ecological niches. Within  
20 module connectivity ( $Z_i$ ) and among-module connectivity ( $P_i$ ) indexes were used to identify key module  
21 members (Olesen *et al.*, 2007, Fig. 6). In an ecological context, the peripherals may represent specialists,  
22 while module hubs and connectors may be more considered as intra-module and inter-module generalists



1 respectively. Network hubs are usually considered as super-generalists (Deng et al., 2012). It is interesting  
2 that the numbers of connectors that are considered as generalists were reduced whereas module hubs  
3 were increased under the HC treatment. However, two network hubs, the super-generalists that are more  
4 important than module hubs and connectors, were detected in the LC network but not in the HC network  
5 (Fig. 6).

#### 6 **4 Discussion**

7 Although effects of elevated CO<sub>2</sub> on bacterioplankton communities have been reported (Allgaier et al.,  
8 2008; Tanaka *et al.*, 2008; Wang et al., 2016; Zhang et al., 2013; Ray et al., 2012; Roy et al., 2013;  
9 Baltar et al., 2015), how marine bacteria communities react to the occurrence of elevated CO<sub>2</sub> combined  
10 with other environmental perturbations is still uncertain. This mesocosm study comprehensively  
11 investigated the effects of elevated CO<sub>2</sub> on bacterioplankton community structure and networks using  
12 Illumina sequencing and ecological network analysis. The results indicate that the abundance and the  
13 community structure at different taxonomic levels were generally similar at different diatom bloom  
14 stages between the HC and LC treatment, in line with previous ocean acidification mesocosm  
15 bacterioplankton community studies (Tanaka *et al.*, 2008; Wang et al., 2016; Zhang et al., 2013; Ray et  
16 al., 2012; Roy et al., 2013; Baltar et al., 2015). The difference in bacterioplankton community diversity  
17 between the HC and LC treatments was also not remarkable as well. These results suggest the possibility  
18 that the whole bacterioplankton community has a certain degree of resilience to elevated CO<sub>2</sub>, which is  
19 consistent with a previous stated hypothesis (Joint et al., 2011).

20 It has previously been proposed that the observed insignificant effects of ocean acidification on coastal  
21 bacterioplankton and their resilience to elevated CO<sub>2</sub> was due to their adaptation to strong natural  
22 variability in pH, with amplitudes of >0.3 units from diel fluctuation and seasonal dynamics found in



1 coastal ecosystems (Hofmann et al., 2011). The comparative ecological network analysis in this study to  
2 some extent explains the resilience of the bacterioplankton community to elevated CO<sub>2</sub> levels. According  
3 to the present study, substantial amount of OTUs that were sparsely distributed in different and small  
4 modules in the LC network became connected with each other and formed less numbers of modules in  
5 the HC network, implying elevated CO<sub>2</sub> has the potential to reassemble the bacterioplankton community  
6 (Fig. 5). The positive relationship among these principle components were almost unaltered in the  
7 network analysis, suggesting that elevated CO<sub>2</sub> did not change the network of principal components of  
8 bacterioplankton and the positive relationship among them were vital for the whole bacterioplankton  
9 community's stability (Fig. 5).

10 It was also reported that sparsely distributed fungal species were reassembled into highly connected  
11 dense modules under long-term elevated CO<sub>2</sub> conditions (Tu et al., 2015). It is noteworthy that the OTUs  
12 involved in possible community reassembly were not very abundant, whereas the relationship between  
13 the abundant OTUs was virtually unaltered by elevated CO<sub>2</sub> in this study. Although elevated CO<sub>2</sub>  
14 promoted the reassembly of the bacterioplankton community, the network constructed by abundant  
15 OTUs which are usually considered as the foundation of the whole bacterioplankton community was still  
16 stable in response to elevated CO<sub>2</sub>. This to some extent led to the stability of the bacterioplankton  
17 community under the ocean acidification stimuli in the context of eutrophic conditions in the current  
18 study. Additionally, this data indicates that more negative than positive relationships between OTUs  
19 were observed in both HC and LC treatments, which is consistent with a previous ocean acidification  
20 mesocosm study conducted in the Arctic Ocean (Wang et al., 2016). It was proposed that a community  
21 with more competitors would be more stable and yield less variation under environmental fluctuations  
22 (Gonzalez and Loreau, 2009). So, it could be speculated that the dominant competition relationship





1 between bacterioplankton species in this mesocosm experiment helped the whole bacterioplankton  
2 community to adapt to pH perturbations, with less variation in total biomass and diversity.

3 Although the effects of elevated CO<sub>2</sub> on bacterioplankton community structure were not significant,  
4 the proportion of some groups of bacterioplankton varied between the HC and LC treatments in the early  
5 stages of the diatom bloom. Elevated CO<sub>2</sub> significantly increased the proportion of Flavobacteriia  
6 dominated by Flavobacteriales, in the HC treatment on day 10 when the diatoms cells began to grow  
7 rapidly. In contrast, the HC treatment had negative effects on the growth of Alphaproteobacteria  
8 compared to the LC treatment. The results reported here are in line with previous reports about the  
9 response of Flavobacteriia to ocean acidification in biofilm and single species experiments (Witt et al.,  
10 2011; Teira *et al.*, 2012). Flavobacteriia are considered as the “first responders” to phytoplankton blooms  
11 because they specialize in attacking algal cells and further degrading biopolymers and organic matter  
12 derived from algal detrital particles (Kirchman, 2002; Teeling *et al.*, 2012). Flavobacteriia are especially  
13 good at converting high molecular weight (HMW) dissolved organic matter (DOM) to low molecular  
14 weight (LMW) DOM using the highly efficient, extracellular, multi-protein complex TonB-dependent  
15 transporter (TBDT) system based on previous in situ proteomics and metatranscriptomics data (Teeling  
16 *et al.*, 2012). Higher abundance of Flavobacteriia under elevated CO<sub>2</sub> means more HMW DOM could be  
17 degraded and so enter into the carbon cycle (Buchan *et al.*, 2014). Based on the results reported here, it  
18 can be speculated that increased amounts of Flavobacteriia under the elevated CO<sub>2</sub> treatment combined  
19 with eutrophication could promote the TBDT system to break down HMW DOM and lead to improved  
20 efficiency of the Microbial Carbon Pump (MCP), and possibly further influence the carbon storage in the  
21 ocean (Jiao *et al.*, 2010).

22 Additionally, it has been postulated that the Flavobacteriia originated light-driven proton pump



1 proteorhodopsin could be involved in dealing with ocean acidification and pH perturbation (Fuhrman et  
2 al., 2008). Recent metatranscriptomic data further emphasize the role of proteorhodopsin in pH  
3 homeostasis in bacterioplankton under elevated CO<sub>2</sub> (Bunse *et al.*, 2016; Gómez-Consarnau *et al.*, 2007).  
4 In this study, we speculate that the stimulated growth of Flavobacteria could have been due to the  
5 enhanced activation of proteorhodopsin under the HC treatment at the early stage of diatom bloom. The  
6 mechanisms of proteorhodopsin in pH homeostasis in bacterioplankton under elevated CO<sub>2</sub> need further  
7 investigation in the future.

8 Interestingly, Flavobacteria in our study showed higher abundance in the HC treatment in the early  
9 phytoplankton bloom stage. However, a negative relationship between CO<sub>2</sub> level and relative abundance  
10 of Bacteroidetes based on terminal restriction fragment length polymorphism (T-RFLP) method was  
11 observed in a mesocosm experiment conducted in the Arctic region with low nutrient levels (Roy *et al.*,  
12 2013). Moreover, the effects of elevated CO<sub>2</sub> on bacterioplankton community interaction webs in this  
13 study were not observed in a previous mesocosm experiment conducted in the Arctic Ocean (Wang *et al.*,  
14 2016; Roy *et al.*, 2013).

## 15 **Conclusion**

16 Briefly, elevated CO<sub>2</sub> was not a strong influence on bacterioplankton community structure, compared  
17 to the diatom bloom process based on 16S V3-V4 region Illumina sequencing. We also found that the  
18 elevated CO<sub>2</sub> appeared to reassemble the community network of taxa present with low abundance but  
19 hardly altered the network structure of the bacterioplankton taxa present with high abundance based on  
20 ecological network analysis. The results showed that the effects of elevated CO<sub>2</sub> in the context of  
21 eutrophication in the current study were different compared to elevated CO<sub>2</sub> on bacterioplankton  
22 community networks in mesocosm study carried out in the oligotrophic Arctic Ocean. The data here and



1 previous reported seemingly contradictory results highlight the importance of including the combined  
2 effects of ocean acidification and other anthropogenic perturbations to interpret and predict the impact of  
3 global change on marine life.

4 In this study, a simplified model phytoplankton community was used, so two diatom species *P.*  
5 *tricornutum* and *T. weissflogii* dominated in both LC and HC treatments. It is possible that the similarity  
6 of the two bacterial communities in the two treatments was due to the similar composition and quality of  
7 DOM produced by these two diatoms. With a more diverse natural phytoplankton community  
8 experimental system, perhaps different phytoplankton taxa would have dominated in the HC and LC  
9 treatments, leading to different bacterial communities.

#### 10 **Author contributions**

11 Conceived and designed the experiments: K.G., X.L., M.D.. Performed the experiments: R.P.H., X.L.,  
12 Y.P.W., Y.L.. Analysed data: R.P.H. and X.L.. Wrote the paper: X.L.. Revised the paper: D.H. and K.G.  
13 All authors reviewed the manuscript.

#### 14 **Acknowledgments**

15 This study was supported by the National Key Research and Development Program of China (Grant No.  
16 2016YFA0601302), the National Natural Science Foundation of China (No. 41306096 to XL, No.  
17 41430967 and No. 41120164007 to KG), State Oceanic Administration of China  
18 (SOA, GASI-03-01-02-04), The Open Fund of Key Laboratory of Marine Ecology and Environmental  
19 Sciences, Institute of Oceanology, Chinese Academy of Sciences, and Laboratory of Marine Ecology  
20 and Environmental Science, Qingdao National Laboratory for Marine Science and Technology  
21 (KLMEES201608), Joint project of NSFC and Shandong province (Grant No. U1406403), Strategic



1 Priority Research Program of Chinese Academy of Sciences (Grant No. XDA11020302). DAH's  
2 contributions were supported by U.S. NSF OCE 1260490 and 1538525, and their visits to Xiamen were  
3 supported by “111” project from the Ministry of Education.

#### 4 **Competing interests:**

5 The authors declare no competing financial interests.

#### 6 **Reference**

- 7 Allgaier, M., Riebesell, U., Vogt, M., Thyraug, R. and Grossart, H.-P.: Coupling of heterotrophic  
8 bacteria to phytoplankton bloom development at different pCO<sub>2</sub> levels: a mesocosm study,  
9 Biogeosciences, 5(4), 1007–1022, doi:10.5194/bgd-5-317-2008, 2008.
- 10 Anderson, M. J.: A new method for non-parametric multivariate analysis of variance, Austral Ecol.,  
11 26(2001), 32–46, doi:10.1046/j.1442-9993.2001.01070.x, 2001.
- 12 Azam, F.: Microbial control of oceanic carbon flux: the plot thickens., Science (80-. ), 280(5364),  
13 694–696, 1998.
- 14 Baltar, F., Palovaara, J., Vila-Costa, M., Salazar, G., Calvo, E., Pelejero, C., Marras é C., Gasol, J. M.  
15 and Pinhassil, J.: Response of rare, common and abundant bacterioplankton to anthropogenic  
16 perturbations in a Mediterranean coastal site, FEMS Microbiol. Ecol., 91(6), 1–12,  
17 doi:10.1093/femsec/fiv058, 2015.
- 18 Buchan, A., LeClerc, G. R., Gulvik, C. A. and González, J. M.: Master recyclers: features and functions  
19 of bacteria associated with phytoplankton blooms, Nat. Rev. Microbiol., 12(10), 686–698,  
20 doi:10.1038/nrmicro3326, 2014.
- 21 Bunse, C., Lundin, D., Karlsson, C. M. G., Vila-Costa, M., Palovaara, J., Akram, N., Svensson, L.,



- 1 Holmfeldt, K., González, J. M., Calvo, E., Pelejero, C., Marras, C., Dopson, M., Gasol, J. M. and  
2 Pinhassi, J.: Response of marine bacterioplankton pH homeostasis gene expression to elevated  
3 CO<sub>2</sub>, *Nat. Clim. Chang.*, (January), doi:10.1038/nclimate2914, 2016.
- 4 Busch, D. S., O'Donnell, M. J., Hauri, C., Mach, K. J., Poach, M., Doney, S. C. and Signorini, S. R.:  
5 Understanding, characterizing, and communicating responses to ocean acidification: Challenges  
6 and uncertainties, *Oceanography*, 28(2), 30–39, doi:http://dx.doi.org/10.5670/oceanog.2015.29,  
7 2015.
- 8 Cai, W.-J., Hu, X., Huang, W.-J., Murrell, M. C., Lehrter, J. C., Lohrenz, S. E., Chou, W.-C., Zhai, W.,  
9 Hollibaugh, J. T., Wang, Y., Zhao, P., Guo, X., Gundersen, K., Dai, M. and Gong, G.-C.:  
10 Acidification of subsurface coastal waters enhanced by eutrophication, *Nat. Geosci.*, 4(11), 766–  
11 770, doi:10.1038/ngeo1297, 2011.
- 12 Caporaso, J. G., Kuczynski, J., Stombaugh, J., Bittinger, K., Bushman, F. D., Costello, E. K., Fierer, N.,  
13 Peña, A. G., Goodrich, J. K., Gordon, J. I., Huttley, G. a, Kelley, S. T., Knights, D., Koenig, J. E.,  
14 Ley, R. E., Lozupone, C. a, McDonald, D., Muegge, B. D., Pirrung, M., Reeder, J., Sevinsky, J. R.,  
15 Turnbaugh, P. J., Walters, W. a, Widmann, J., Yatsunenko, T., Zaneveld, J. and Knight, R.:  
16 correspondence QIIME allows analysis of high- throughput community sequencing data Intensity  
17 normalization improves color calling in SOLiD sequencing, *Nat. Publ. Gr.*, 7(5), 335–336,  
18 doi:10.1038/nmeth0510-335, 2010.
- 19 Clarke, K. R.: Non-parametric multivariate analyses of changes in community, *Aust. J. Ecol.*, (18),  
20 117–143, 1993.
- 21 Deng, Y., Jiang, Y.-H., Yang, Y., He, Z., Luo, F. and Zhou, J.: Molecular ecological network analyses,  
22 *BMC Bioinformatics*, 13, 113, doi:10.1186/1471-2105-13-113, 2012.



- 1 Falkowski, P. G., Fenchel, T. and Delong, E. F.: The Microbial Engines That Drive Earth's  
2 Biogeochemical Cycles, *Science* (80-. ), 320(5879), 1034–1039, doi:10.1126/science.1153213,  
3 2008.
- 4 Francis, C. A., Roberts, K. J., Beman, J. M., Santoro, A. E. and Oakley, B. B.: Ubiquity and diversity  
5 of ammonia-oxidizing archaea in water columns and sediments of the ocean, , 102(41), 14683–  
6 14688, doi:10.1073/pnas.0506625102, 2005.
- 7 Fuhrman, J. a, Schwalbach, M. S. and Stingl, U.: Proteorhodopsins: an array of physiological roles?,  
8 *Nat. Rev. Microbiol.*, 6(6), 488–494, doi:10.1038/nrmicro1893, 2008.
- 9 Gattuso, J.-P., Magnan, A., Bille, R., Cheung, W. W. L., Howes, E. L., Joos, F., Allemand, D., Bopp,  
10 L., Cooley, S. R., Eakin, C. M., Hoegh-Guldberg, O., Kelly, R. P., Portner, H.-O., Rogers, a. D.,  
11 Baxter, J. M., Laffoley, D., Osborn, D., Rankovic, A., Rochette, J., Sumaila, U. R., Treyer, S. and  
12 Turley, C.: Contrasting futures for ocean and society from different anthropogenic CO<sub>2</sub> emissions  
13 scenarios, *Science* (80-. ), 349(6243), aac4722-1-aac4722-10, doi:10.1126/science.aac4722, 2015.
- 14 Gómez-Consarnau, L., González, J. M., Coll-Lladó M., Gourdon, P., Pascher, T., Neutze, R.,  
15 Pedró-Alió C. and Pinhassi, J.: Light stimulates growth of proteorhodopsin-containing marine  
16 Flavobacteria, *Nature*, 445(7124), 210–213, doi:10.1038/nature05381, 2007.
- 17 Gonzalez, A. and Loreau, M.: The Causes and Consequences of Compensatory Dynamics in Ecological  
18 Communities, *Annu. Rev. Ecol. Evol. Syst.*, 40(1), 393–414,  
19 doi:10.1146/annurev.ecolsys.39.110707.173349, 2009.
- 20 Guidi, L., Chaffron, S., Bittner, L., Eveillard, D., Larhlimi, A., Roux, S., Darzi, Y., Audic, S., Berline,  
21 L., Brum, J., Coelho, L. P., Espinoza, J. C. I., Malviya, S., Sunagawa, S., Dimier, C.,  
22 Kandels-Lewis, S., Picheral, M., Poulain, J., Searson, S., Coordinators, T. O., Stemmann, L., Not,



- 1 F., Hingamp, P., Speich, S., Follows, M., Karp-Boss, L., Boss, E., Ogata, H., Pesant, S.,  
2 Weissenbach, J., Wincker, P., Acinas, S. G., Bork, P., de Vargas, C., Iudicone, D., Sullivan, M. B.,  
3 Raes, J., Karsenti, E., Bowler, C. and Gorsky, G.: Plankton networks driving carbon export in the  
4 oligotrophic ocean, *Nature*, 532(7600), in review, doi:10.1038/nature16942, 2015.
- 5 Hofmann, G. E., Smith, J. E., Johnson, K. S., Send, U., Levin, L. A., Micheli, F., Paytan, A., Price, N.  
6 N., Peterson, B., Takeshita, Y., Matson, P. G., Crook, E. D., Kroeker, K. J., Gambi, M. C., Rivest,  
7 E. B., Frieder, C. A., Yu, P. C. and Martz, T. R.: High-Frequency Dynamics of Ocean pH: A  
8 Multi-Ecosystem Comparison, *PLoS One*, 6(12), e28983, doi:10.1371/journal.pone.0028983,  
9 2011.
- 10 Jiao, N., Herndl, G. J., Hansell, D. A., Benner, R., Kattner, G., Wilhelm, S. W., Kirchman, D. L.,  
11 Weinbauer, M. G., Luo, T., Chen, F. and Azam, F.: Microbial production of recalcitrant dissolved  
12 organic matter: long-term carbon storage in the global ocean, *Nat. Rev. Microbiol.*, 8(8), 593–599,  
13 doi:10.1038/nrmicro2386, 2010.
- 14 Jin, P., Wang, T., Liu, N., Dupont, S., Beardall, J., Boyd, P. W., Riebesell, U. and Gao, K.: Ocean  
15 acidification increases the accumulation of toxic phenolic compounds across trophic levels., *Nat.*  
16 *Commun.*, 6(October), 8714, doi:10.1038/ncomms9714, 2015.
- 17 Joint, I., Doney, S. C. and Karl, D. M.: Will ocean acidification affect marine microbes?, *ISME J.*, 5(1),  
18 1–7, doi:10.1038/ismej.2010.79, 2011.
- 19 Kirchman, D. L.: The ecology of Cytophaga-Flavobacteria in aquatic environments, *FEMS Microbiol.*  
20 *Ecol.*, 39(2), 91–100, doi:10.1016/S0168-6496(01)00206-9, 2002.
- 21 Krause, E., Wichels, A., Giménez, L., Lunau, M., Schilhabel, M. B. and Gerds, G.: Small Changes in  
22 pH Have Direct Effects on Marine Bacterial Community Composition: A Microcosm Approach,



- 1 PLoS One, 7(10), e47035, doi:10.1371/journal.pone.0047035, 2012.
- 2 Labare, M. P., Bays, J. T., Butkus, M. a., Snyder-Leiby, T., Smith, A., Goldstein, A., Schwartz, J. D.,  
3 Wilson, K. C., Ginter, M. R., Bare, E. a., Watts, R. E., Michealson, E., Miller, N. and LaBranche,  
4 R.: The effects of elevated carbon dioxide levels on a *Vibrio* sp. isolated from the deep-sea,  
5 Environ. Sci. Pollut. Res., 17(4), 1009–1015, doi:10.1007/s11356-010-0297-z, 2010.
- 6 Lewis, E., and D. W. R. Wallace: Program developed for CO<sub>2</sub> system calculations, Rep.  
7 ORNL/CDIAC-105, Carbon Dioxide Inf. Anal. Cent., Oak Ridge Natl. Lab., Oak Ridge, Tenn.,  
8 doi:10.2172/639712, 1998.
- 9 Lidbury, I., Johnson, V., Hall-spencer, J. M., Munn, C. B. and Cunliffe, M.: Community-level response  
10 of coastal microbial biofilms to ocean acidification in a natural carbon dioxide vent ecosystem,  
11 Mar. Pollut. Bull., 64(5), 1063–1066, doi:10.1016/j.marpolbul.2012.02.011, 2012.
- 12 Lima-Mendez, G., Faust, K., Henry, N., Decelle, J., Colin, S., Carcillo, F., Chaffron, S.,  
13 Ignacio-Espinosa, J. C., Roux, S., Vincent, F., Bittner, L., Darzi, Y., Wang, J., Audic, S., Berline,  
14 L., Bontempi, G., Cabello, A. M., Coppola, L., Cornejo-Castillo, F. M., D’Ovidio, F., De Meester,  
15 L., Ferrera, I., Garet-Delmas, M.-J., Guidi, L., Lara, E., Pesant, S., Royo-Llonch, M., Salazar, G.,  
16 Sanchez, P., Sebastian, M., Souffreau, C., Dimier, C., Picheral, M., Searson, S., Kandels-Lewis, S.,  
17 Gorsky, G., Not, F., Ogata, H., Speich, S., Stemmann, L., Weissenbach, J., Wincker, P., Acinas, S.  
18 G., Sunagawa, S., Bork, P., Sullivan, M. B., Karsenti, E., Bowler, C., de Vargas, C. and Raes, J.:  
19 Determinants of community structure in the global plankton interactome, Science (80-. ),  
20 348(6237), 1262073–1262073, doi:10.1126/science.1262073, 2015.
- 21 Liu, J., Weinbauer, M., Maier, C., Dai, M. and Gattuso, J.: Effect of ocean acidification on microbial  
22 diversity and on microbe-driven biogeochemistry and ecosystem functioning, Aquat. Microb.





- 1 Ecol., 61(3), 291–305, doi:10.3354/ame01446, 2010.
- 2 Liu, N., Tong S., Yi, X., Li, Y., Li, Z., Miao, H., Wang, T., Li F., Yan, D., Huang, R., Wu, Y.,  
3 Hutchins, D., Beardall, J., Dai M., Gao, K.: Carbon assimilation and losses during an ocean  
4 acidification mesocosm experiment, with special reference to algal blooms, submitted.
- 5 McDonald, D., Price, M. N., Goodrich, J., Nawrocki, E. P., DeSantis, T. Z., Probst, A., Andersen, G. L.,  
6 Knight, R. and Hugenholtz, P.: An improved Greengenes taxonomy with explicit ranks for  
7 ecological and evolutionary analyses of bacteria and archaea, ISME J., 6(3), 610–618,  
8 doi:10.1038/ismej.2011.139, 2012.
- 9 Meron, D., Atias, E., Iasur Kruh, L., Elifantz, H., Minz, D., Fine, M. and Banin, E.: The impact of  
10 reduced pH on the microbial community of the coral *Acropora eurystroma*, ISME J., 5(1), 51–60,  
11 doi:10.1038/ismej.2010.102, 2011.
- 12 Mielke, P. W., Berry, K. J., Brockwell, P. J. & Williams, J. S.: A class of nonparametric tests based on  
13 multiresponse permutation procedures, *Biometrika*, (68), 720–724, 1981.
- 14 Ray, J. L., Töpper, B., An, S., Silyakova, A., Spindelböck, J., Thyraug, R., Dubow, M. S., Thingstad,  
15 T. F. and Sandaa, R. A.: Effect of increased pCO<sub>2</sub> on bacterial assemblage shifts in response to  
16 glucose addition in Fram Strait seawater mesocosms, *FEMS Microbiol. Ecol.*, 82(3), 713–723,  
17 doi:10.1111/j.1574-6941.2012.01443.x, 2012.
- 18 Roy, A.-S., Gibbons, S. M., Schunck, H., Owens, S., Caporaso, J. G., Sperling, M., Nissimov, J. I.,  
19 Romac, S., Bittner, L., Mühlhng, M., Riebesell, U., LaRoche, J. and Gilbert, J. a.: Ocean  
20 acidification shows negligible impacts on high-latitude bacterial community structure in coastal  
21 pelagic mesocosms, *Biogeosciences*, 10(1), 555–566, doi:10.5194/bg-10-555-2013, 2013.
- 22 Tanaka, T., Thingstad, T. F., Løvdal, T., Grossart, H.-P., Larsen, A., Schulz, K. G. and Riebesell, U.:



- 1        Availability of phosphate for phytoplankton and bacteria and of labile organic carbon for bacteria  
2        at different pCO<sub>2</sub> levels in a mesocosm study, *Biogeosciences*, (5), 669–678,  
3        doi:10.5194/bgd-4-3937-2007, 2007.
- 4        Teeling, H., Fuchs, B. M., Becher, D., Klockow, C., Gardebrecht, A., Bennke, C. M., Kassabgy, M.,  
5        Huang, S., Mann, A. J., Waldmann, J., Weber, M., Klindworth, A., Otto, A., Lange, J., Bernhardt,  
6        J., Reinsch, C., Hecker, M., Peplies, J., Bockelmann, F. D., Callies, U., Gerdt, G., Wichels, A.,  
7        Wiltshire, K. H., Glockner, F. O., Schweder, T. and Amann, R.: Substrate-Controlled Succession  
8        of Marine Bacterioplankton Populations Induced by a Phytoplankton Bloom, *Science* (80-. ),  
9        336(6081), 608–611, doi:10.1126/science.1218344, 2012.
- 10      Teira, E., Fernández, A., Álvarez-Salgado, X. A., García-Martín, E. E., Serret, P. and Sobrino, C.:  
11      Response of two marine bacterial isolates to high CO<sub>2</sub> concentration, *Mar. Ecol. Prog. Ser.*, 453,  
12      27–36, doi:10.3354/meps09644, 2012.
- 13      Tu, Q., Yuan, M., He, Z., Deng, Y., Xue, K., Wu, L., Hobbie, S. E., Reich, P. B. and Zhou, J.: Fungal  
14      Communities Respond to Long-Term CO<sub>2</sub> Elevation by Community Reassembly, *Appl. Environ.*  
15      *Microbiol.*, 81(7), 2445–2454, doi:10.1128/AEM.04040-14, 2015.
- 16      Wang, Y., Zhang, R., Zheng, Q., Deng, Y., Van Nostrand, J. D., Zhou, J. and Jiao, N.:  
17      Bacterioplankton community resilience to ocean acidification: evidence from microbial network  
18      analysis, *ICES J. Mar. Sci.*, 73(3), 865–875, doi:10.1093/icesjms/fst176, 2016.
- 19      Witt, V., Wild, C., Anthony, K. R. N., Diaz-Pulido, G. and Uthicke, S.: Effects of ocean acidification  
20      on microbial community composition of, and oxygen fluxes through, biofilms from the Great  
21      Barrier Reef, *Environ. Microbiol.*, 13(11), 2976–2989, doi:10.1111/j.1462-2920.2011.02571.x,  
22      2011.



- 1 Zhang, J., Kobert, K., Flouri, T. and Stamatakis, A.: PEAR: a fast and accurate Illumina Paired-End
- 2 reAd mergeR, *Bioinformatics*, 30(5), 614–620, doi:10.1093/bioinformatics/btt593, 2014.
- 3 Zhang, R., Xia, X., Lau, S. C. K., Motegi, C., Weinbauer, M. G. and Jiao, N.: Response of
- 4 bacterioplankton community structure to an artificial gradient of pCO<sub>2</sub> in the Arctic Ocean,
- 5 *Biogeosciences*, 10(6), 3679–3689, doi:10.5194/bg-10-3679-2013, 2013.
- 6 Zhou, J., Deng, Y., Luo, F., He, Z., Tu, Q. and Zhi, X.: Functional molecular ecological networks,
- 7 *MBio*, 1(4), e00169-10, doi:10.1128/mBio.00169-10.Editor, 2010.
- 8
- 9
- 10
- 11
- 12
- 13
- 14
- 15
- 16
- 17
- 18
- 19
- 20
- 21
- 22



## 1 **Figure legends**

2 **Figure 1** Location of the FOANIC-XMU (Facility for the Study of Ocean Acidification Impacts of  
3 Xiamen University) mesocosm platform (Wuyuan Bay, Xiamen, Fujian province, East China Sea  
4 (N24°31'48",  
5 E118°10'47")).

6  
7 **Figure 2** Temporal variations of  $p\text{CO}_2$  and Chl $a$  during the whole experiment. The  $p\text{CO}_2$  was calculated  
8 from DIC and pH by CO2SYS Program (Lewis et al. 1998).

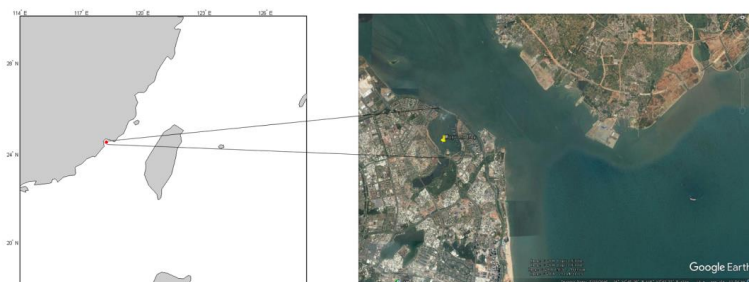
9  
10 **Figure 3** Bacterioplankton community structure overview at different taxonomic levels during day 4, 6,  
11 8, 10, 13, 19 and 29 under LC and HC. X-axis represents sample name (for example, D4. 1 refers to  
12 bacterioplankton in mesocosm bag 1 collected on day 4) and the Y-axis represents relative abundance of  
13 different groups of bacterioplankton.

14  
15 **Figure 4** The relative abundance over time of primary taxa of the bacterioplankton community; HC (2, 4,  
16 7 mesocosm bags) in red and LC (1, 6, 8 mesocosm bags) in black. Data are the means  $\pm$  SD,  
17 Proteobacteria (a) and Bacteroidetes (b) are phylum level; Flavobacteriia (c) and Alphabacteria (d) are  
18 class level; Flavobacteriales (e) and Rhodobacteriales (f) are order level; Flavobacteriaceae (g) and  
19 Rhodobacteraceae (h) are family level. The asterisk represents a difference at  $p < 0.05$ .

20  
21 **Figure 5** Bacterioplankton network interactions under LC (a) and HC (b) conditions. Each node  
22 represents an OUT. Node colors demonstrate different taxon. Each line connects two OTUs. A blue line



1 indicate a negative interaction between nodes suggesting a predation or competition while a red line  
2 indicates a positive interaction suggesting mutualism or cooperation. OTUs with importance are marked  
3 with OTU identification numbers.  
4  
5 **Figure 6** Sub-modules in ecological network analysis under LC (a) and HC (b) conditions. Each dot  
6 represents an OTU. The  $Z$ - $P$  plot shows OTU distribution based on their module-based topological role  
7 according to within-module ( $Z$ ) and among-module ( $P$ ) connectivity. The nodes were defined as module  
8 hubs with  $Z_i > 2.5$  and  $P_i < 0.625$ , which were more closely connected within the module, while the  
9 connectors were nodes with  $Z_i < 2.5$  and  $P_i > 0.625$  were more closely connected to nodes in other  
10 modules. Network hubs are super-generalist with a  $Z_i > 2.5$  and  $P_i > 0.625$ . The other nodes were  
11 considered peripheral.  
12  
13  
14  
15  
16  
17  
18  
19  
20  
21  
22



1  
2  
3  
4  
5  
6  
7  
8  
9  
10  
11  
12  
13  
14  
15  
16

**Figure 1**

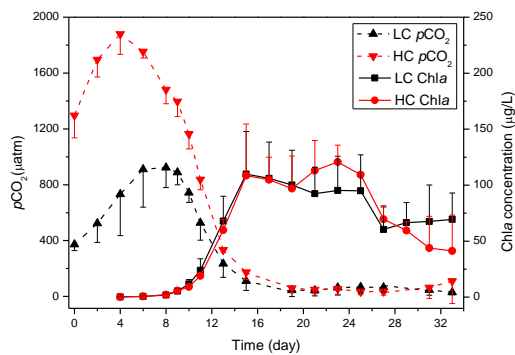
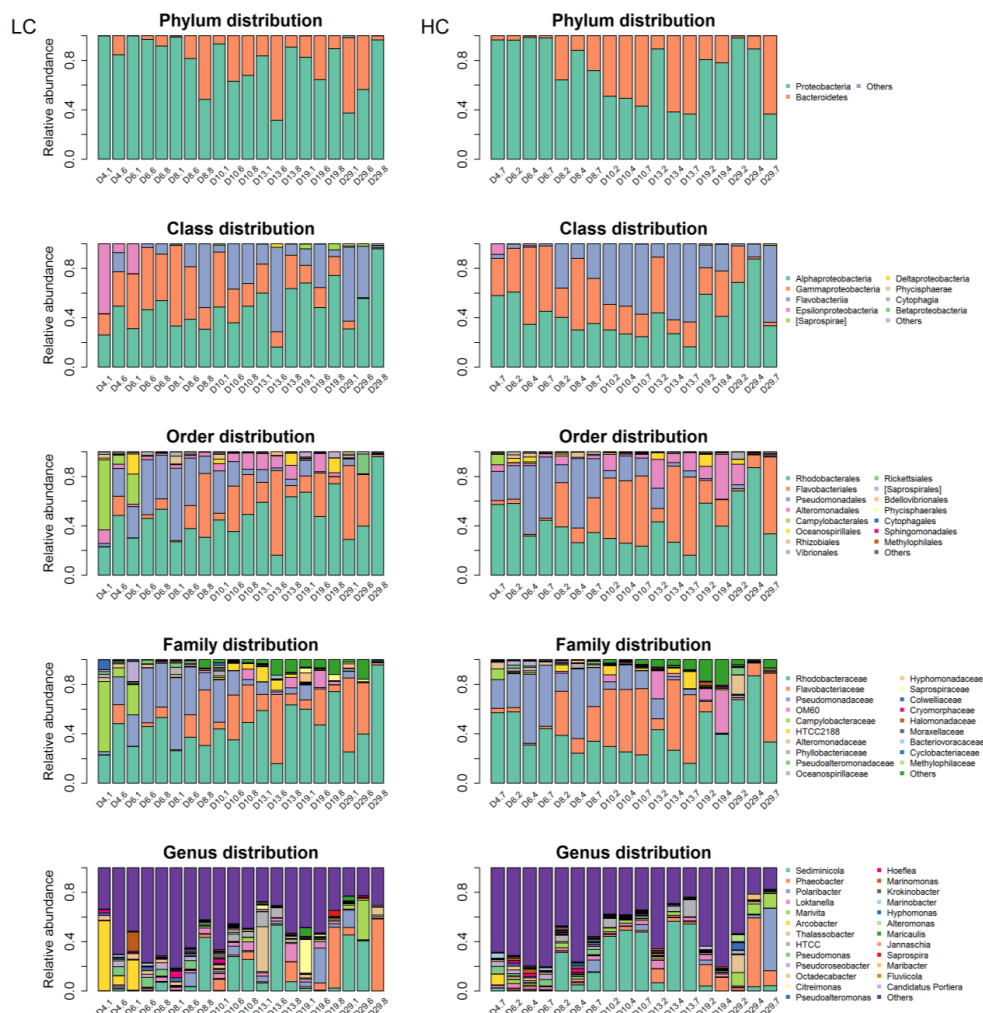


Figure 2

1  
2  
3  
4  
5  
6  
7  
8  
9  
10  
11  
12  
13  
14  
15  
16  
17



1

2

Figure 3



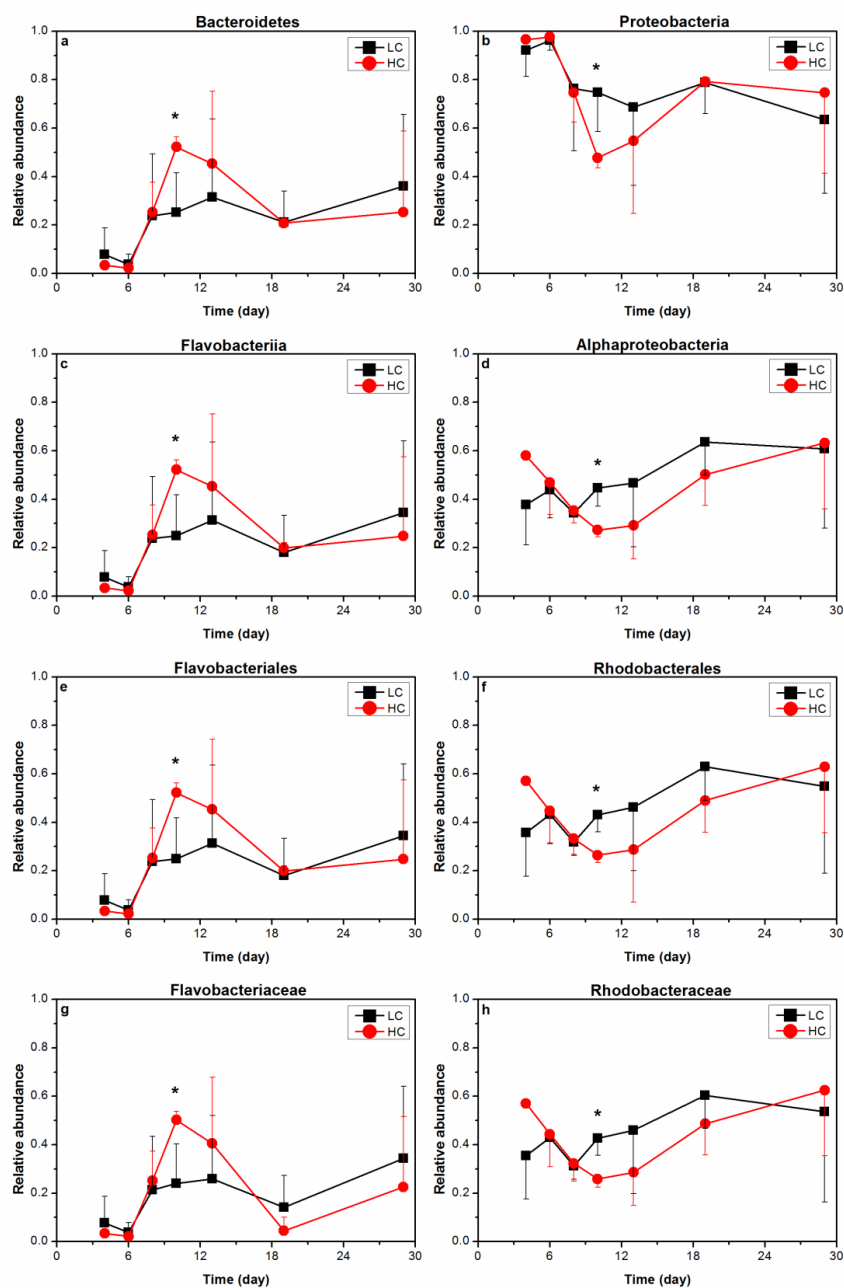


Figure 4

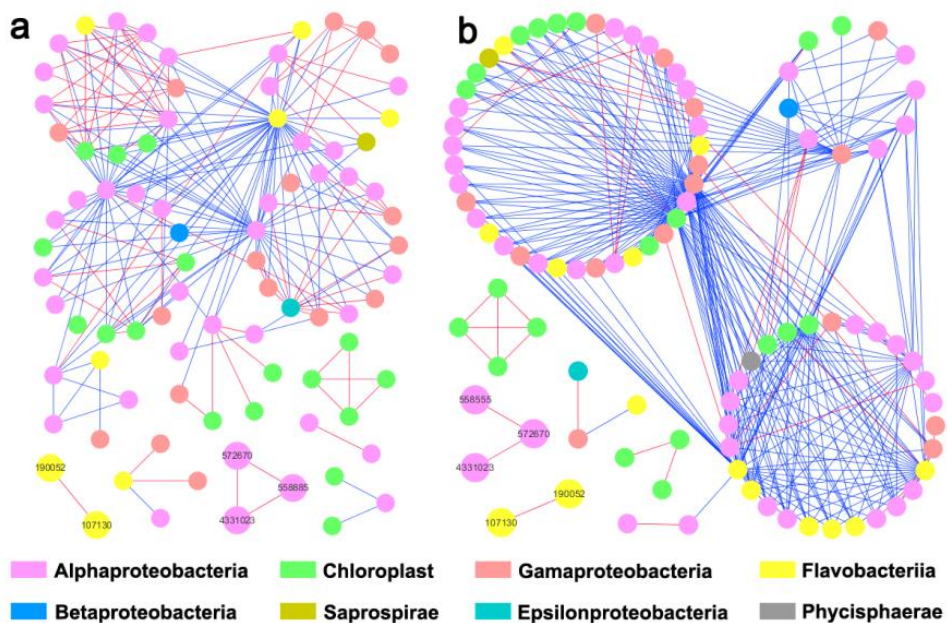


Figure 5

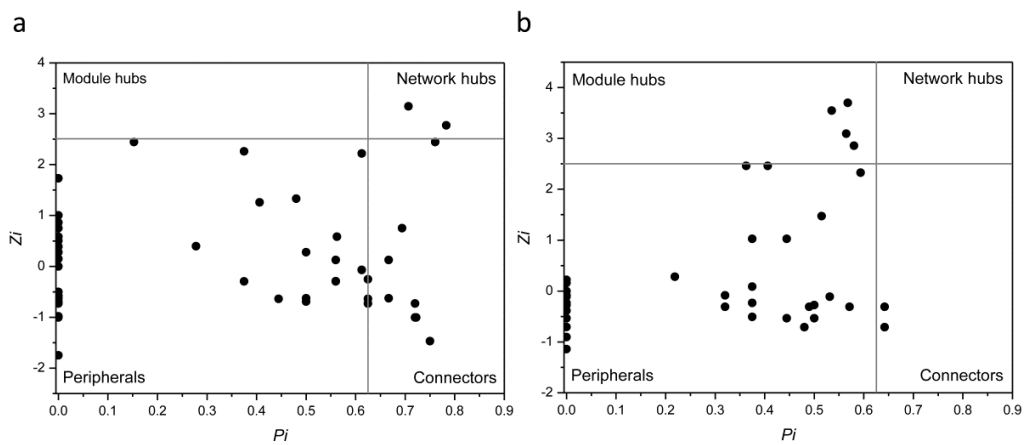


Figure 6



**Table 1** Topological properties of the bacterioplankton communities as represented by molecular networks under HC and LC treatments; also their rewired random networks.

	Experimental network					Random network				
	Total nodes	Total links	R2 of power-law	Average clustering coefficient (avgCC)	Average connectivity	Harmonic geodesic distance (HD)	Modularity	Average clustering coefficient (avgCC)	Harmonic geodesic distance (HD)	Modularity
<b>LC</b>	85	209	0.817	0.402	0.625	3.397	0.414	0.424 +/- 0.023	2.187 +/- 0.049	0.249 +/- 0.010
<b>HC</b>	96	310	0.817	0.448	0.714	2.956	0.303	0.292 +/- 0.023	2.306 +/- 0.059	0.323 +/- 0.008

**Table 2** Dissimilarity tests of bacterial communities under HC and LC treatment at various time points.

Time	Anosim		MRPP		Adonis	
	R	P-value	$\delta$	P-value	R <sup>2</sup>	P
<b>day6</b>	-0.111	0.602	0.3952	1	0.15447	1
<b>day8</b>	0.111	0.284	0.438	0.6	0.2	0.5
<b>day10</b>	0.037	0.613	0.4929	0.7	0.17829	0.7
<b>day13</b>	0.111	0.309	0.412	0.5	0.19714	0.5
<b>day19</b>	0	0.693	0.4336	0.3	0.28263	0.3
<b>day29</b>	-0.259	1	0.4513	0.9	0.15517	0.9

1  
2  
3  
4  
5  
6  
7  
8  
9  
10  
11  
12  
13

14  
15